

## X-ray properties of RL AGN 3C111: detailed case-study

E. Fedorova, B.I. Hnatyk, V.I. Zhdanov

3C111 is a broad line radio galaxy with signatures of FSRQ and Seyfert type disk corona in X-ray spectrum. We use all X-ray data publicly accessible in INTEGRAL, XMM-Newton, SWIFT and Suzaku database to recover the contribution of thermal disk corona emission and nonthermal SSC quasar jet emission to the total X-ray spectrum of 3C111. We show that both components are time-variable what results in variability of equivalent widths (EWs) of Fe lines. From observational data set on EWs of Fe lines and total spectral fluxes of continuum emission at  $E=6.4$  keV for different observational periods, we recover parameters of disk corona and jet spectra. Future investigation of polarization of 3C111 in IR-optical band, where synchrotron emission of jet dominates, could constrain the parameters of SSC emission in 3C111 and improve the disk corona model.

### 3C 111: short info

- Redshift  $z = 0.0485$  [1]
- Broad Line Radio Galaxy [2]
- S1 type AGN [3]
- One-side jet (78 kpc long) [2]
- FR I radio source [2]
- Thermal-dominated spectrum + iron lines [4]
- the value of high-energy exponential cut-off in the RXTE X-ray spectrum is ... () -> too high for an RL AGN, possibly due to jet contamination [5]

Main points:

1. To clear out the "peculiarity" of the X-ray spectrum (high value of the high-energy cut-off)
2. Distinguishing the primary nuclear and jet counterparts in the spectrum, using two ways (and comparing them):
  - Extrapolation of the radio spectrum for jet: we suppose that the photon index of the spectra of the jet base is the same in radio and in X-rays [6, 7]
  - Using the line-continuum connection: we take into account that there is a correlation between the primary continuum flux and Fe-K emission lines intensity

The data used:

- XMM-Newton/EPIC (2002, 2009)
- Suzaku/XIS (2008, 2010)
- Swift/XRT and BAT (2007, 2009, 2010, 2012, 2013, 2017)
- INTEGRAL/ISGRI (2008-2010, 2012, 2013, 2015-2017)
- PLANCK (in radio)

Model used:

- mekal (thermal emission of the disk) with equivalent temperature  $kT$ ;
- pexrav (reflected power-law emission = comptonized emission of the corona, with photon index  $\Gamma_1$ , reflection coefficient  $R$  and exponential cut-off at high energies  $E_c$ );
- po (power-law jet emission, photon index  $\Gamma_2$ );
- zgauss (Fe-K $\alpha$  emission line at 6.4 keV, with the parameters: line energy  $E_{\text{line}}$ , width  $\sigma$  and equivalent width  $EW$ );
- phabs (weak proper/galactic absorption, with column density  $N_H$ ).
- gabs (Gaussian absorption line)

### 1. Extrapolation method:

From the PLANCK spectrum of 3C 111:  $\Gamma=1.66\pm 0.06$

This value was used as frozen for the jet contribution

### 2. Continuum -line connection method:

Analyzing the 5-7 keV full flux dependence vs. equivalent width of 6.4 keV iron emission line. Supposing that there is a linear dependence between them:  $F_{5-7\text{nucl}}=k*EW$ , we can find the lowest value of  $k$  from the set of data (under the condition of the line detection).

## Fitting results:

Dates	kT, keV	N <sub>h1</sub>	Γ <sub>jet</sub>	N <sub>h2</sub>	Γ <sub>cont</sub>	Ec	R	N <sub>h3</sub>	K	Chisq/d.o.f	Flux <sub>5-7</sub> , 10 <sup>12</sup> erg/sm*s	Flux <sub>jet</sub> , 10 <sup>12</sup> erg/sm*s	Flux <sub>cont</sub> , 10 <sup>12</sup> erg/sm*s	E <sub>line</sub> , keV	σ, keV	EW, keV
March 2001	0.18±0.01	4.3±0.6	1.66 (fr)	0.74 <sup>+0.17</sup> <sub>-0.03</sub>	1.92±0.01	-	2.9±0.2	0.8±0.1	-	4688.4/2377	14.7±0.5	12.9	1.82	n/d	-	-
April 2007	1.69 <sup>+1.3</sup> <sub>-0.7</sub> 1.83 <sup>+1.0</sup> <sub>-0.5</sub>	0.8±0.3 0.7±0.4	1.66 (fr) 1.7±0.2	1.2 <sup>+0.8</sup> <sub>-0.4</sub> 1.2±0.5	1.93±0.13 1.92 <sup>+0.09</sup> <sub>-0.07</sub>	158 <sup>+1300</sup> <sub>-100</sub> 275 <sup>+1140</sup> <sub>-220</sub>	0.19±0.19 0.2±0.2	1.2±0.2 1.1±0.2	1.7±0.2 1.7±0.2	719.9/705 719.0/704	6.5±0.3 6.5±0.3	4.2±1.0 5.7±1.0	2.1±1.0 1.0±0.5	6.404 6.404	7*10 <sup>-6</sup> 7*10 <sup>-6</sup>	0.06±0.01 0.07±0.02
Nov 2008	2.5 <sup>+2.9</sup> <sub>-1.3</sub>	<0.3	1.66 (fr)	0.9±0.3	1.62±0.11	440 <sup>+410</sup> <sub>-230</sub>	Unconstr.	0.9±0.3	0.4 <sup>+0.2</sup> <sub>-0.1</sub>	114.1/96	12.0±0.5	12.0±0.5	-	n/d	-	-
Jan 2009	1.58±0.50	<0.8	1.66 (fr)	1.0±0.4	1.82 <sup>+0.05</sup> <sub>-0.13</sub>	>330	1.6±1.2	1.12 <sup>+0.31</sup> <sub>-0.22</sub>	0.8±0.2	60/68	10.6±0.6	10.6±0.6	-	n/d	-	-
Feb 2009	n/d	-	1.66(fr)	0.70±0.01	1.63±0.02	>1000	4.6 <sup>+7.0</sup> <sub>-1.9</sub>	0.68±0.01	0.46±0.03	3331.6/2844	11.8±0.1	7.47	4.575	n/d	-	-
Jan 2010	0.37 <sup>+1.11</sup> <sub>-0.25</sub> 0.37 <sup>+1.11</sup> <sub>-0.25</sub>	3.6 <sup>+4.1</sup> <sub>-1.2</sub> 3.6 <sup>+4.1</sup> <sub>-1.2</sub>	1.66 (fr) 1.66±0.08	0.85 <sup>+0.24</sup> <sub>-0.17</sub> 0.85 <sup>+0.24</sup> <sub>-0.17</sub>	1.53 <sup>+0.08</sup> <sub>-0.07</sub> 1.53 <sup>+0.08</sup> <sub>-0.07</sub>	39 <sup>+23</sup> <sub>-15</sub> 39 <sup>+23</sup> <sub>-15</sub>	<0.25 <0.25	0.83 <sup>+0.10</sup> <sub>-0.08</sub> 0.83 <sup>+0.10</sup> <sub>-0.08</sub>	1.3±0.2 1.3±0.2	108.6/100 108.6/99	13.4±0.7 13.4±0.7	6.18 6.18	8.08 8.08	6.35±0.12 6.35±0.12	<0.6 <0.7	0.16±0.02 0.16±0.03
Dec 2012	0.71 <sup>+1.0</sup> <sub>-0.6</sub> 0.71 <sup>+1.2</sup> <sub>-0.6</sub>	2.0 <sup>+2.6</sup> <sub>-1.3</sub> <19.2	1.66 (fr) 1.50 <sup>+0.21</sup> <sub>-0.05</sub>	1.07 <sup>+0.07</sup> <sub>-0.06</sub> 0.83 <sup>+0.07</sup> <sub>-0.06</sub>	1.21 <sup>+0.25</sup> <sub>-0.11</sub> 2.5±0.3	159 <sup>+170</sup> <sub>-130</sub> >88	<0.7 <0.8	<0.82 0.83 <sup>+0.07</sup> <sub>-0.06</sub>	0.63±0.08 0.56±0.07	165.1/144 164.0/143	14.8±0.5 14.6±1.5	12.3 14.3	2.9 2.1	6.38±0.19 6.38±0.26	<0.1 <0.2	0.07±0.01 0.05±0.02
Jan 2013	0	0	1.66 (fr)	0.82±0.11	2.43 <sup>+0.15</sup> <sub>-0.23</sub>	30 <sup>+160</sup> <sub>-20</sub>	>13	1.4 <sup>+0.6</sup> <sub>-0.2</sub>	0.85 <sup>+0.12</sup> <sub>-0.1</sub>	350.5/255	15.4±0.5	11.8	3.6	n/d	-	-
Feb 2013	0.4±0.2 0.5±0.3	<18.0 <20.0	1.66(fr) 1.68 <sup>+0.02</sup> <sub>-0.04</sub>	0.76 <sup>+0.13</sup> <sub>-0.04</sub> 0.76 <sup>+0.15</sup> <sub>-0.05</sub>	n/d n/d	- -	- -	- -	0.5±0.2 0.5±0.2	234.2/231 234.1/230	20.5±1.2 20.1±1.8	20.5±1.2 20.1±1.8	0	n/d	-	-
June 2016*	2.23 <sup>+0.22</sup> <sub>-0.36</sub>	75±10	1.66(fr)	0.89±0.04	1.40±0.01	11 <sup>+5.0</sup> <sub>-0.5</sub>	<0.85	0.89±0.01	0.8±0.1	710.9/705	3.5±0.1	0.2	3.3	6.35±0.09	<0.82	0.0009

\* + absorbtion line: E<sub>abs</sub>=6.30±0.01 keV, σ=0.01±0.001, S=828 and two additional emissions: E<sub>1</sub>=6.13±0.05, E<sub>2</sub>=6.70±0.05, σ<sub>1</sub>=0.04±0.01, σ<sub>2</sub><0.82, EW<sub>1</sub>=0.09 keV, EW<sub>2</sub>=0.03 keV

In green: first method, Γ<sub>jet</sub> is frozen to 1.66

In red: Γ<sub>jet</sub> is free to vary

The coefficient k in the relation F<sub>5-7nuc</sub>=k\*EW can be estimated as the minimum value of F<sub>5-7total</sub>/EW, which for the existing data is 83.75. Note that it give us possibility to estimate the upper limit on the nuclear contribution to the spectrum only.

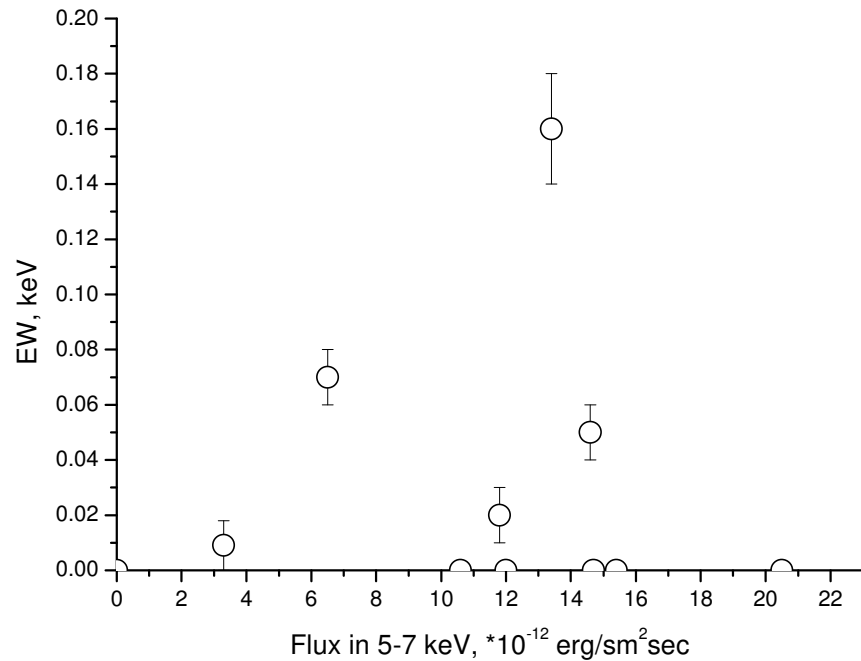


Fig.1 - Fe-Ka EW vs. total 5-7 keV flux

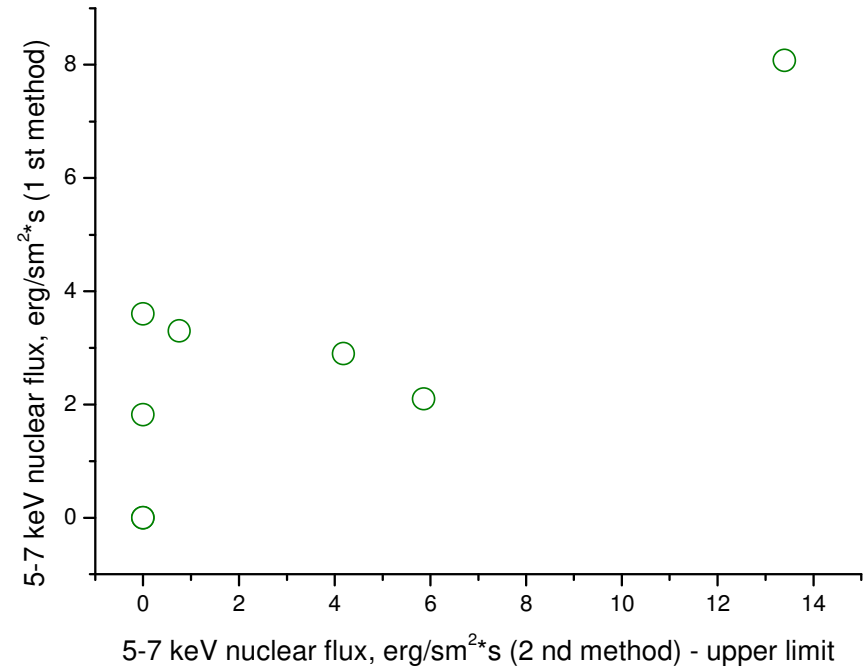


Fig.2 - nuclear flux determined using two methods

### Conclusions:

1. The photon indices of jet power-law emission obtained as a free-to-vary parameters of fitting, are compatible with the value of  $\Gamma=1.66\pm 0.06$  obtained for the PLANCK spectrum. Thus, for this object we can use the extrapolation of the jet base synchrotron emission from the radio to X-rays, which give us possibility to separate the jet and primary nuclear contributions to the X-ray spectrum.

2. The value of high-energy exponential cut-off in the nuclear spectrum, obtained using both methods, are below 100 keV or compatible with this within the error limits. That means that primary nuclear spectrum of 3C 111 in fact does not contradict to the predictions of the spin- or gap-paradigm [8, 9], and the "peculiarity" of its spectrum caused by the jet contamination.
3. The upper limit on the primary nuclear contribution can be estimated using the correlation between the level of continuum nuclear emission and Fe-K emission line intensity.

- [1] A. HEWITT, G. BURBIDGE An optical catalog of extragalactic emission-line objects similar to quasi-stellar objects, *Astrophysical Journal Supplement Series* (ISSN 0067-0049), vol. 75, Feb. 1991, p. 297-356.
- [2] Liu, F. K.; Xie, G. Z. A finding list of extragalactic radio jets and statistical results, *Astronomy and Astrophysics Supplement Series* (ISSN 0365-0138), vol. 95, no. 2, p. 249-268.
- [3] Veron-Cetty, M.-P.; Veron, P. A catalogue of quasars and active nuclei: 12th edition, *Astronomy and Astrophysics*, Volume 455, Issue 2, August IV 2006, pp.773-777
- [4] S. de Jong, V. Beckmann, F. Mattana *Astronomy & Astrophysics*, Volume 545, id.A90, 8 pp.
- [5] E. Fedorova, A. Vasylenko, V. Zhdanov, Peculiar AGNs from the INTEGRAL and RXTE data, *Bulletin of Taras Shevchenko National University of Kyiv. Astronomy*, no. 55, p. 29-34 (2017)
- [6] A. A. Zdziarski, P. Lubiński, M. Gilfanov, M. Revnivtsev, Correlations between X-ray and radio spectral properties of accreting black holes, *Monthly Notices of the Royal Astronomical Society*, Volume 342, Issue 2, 21 June 2003, Pages 355–372, <https://doi.org/10.1046/j.1365-8711.2003.06556.x>
- [7] Miller-Jones, J. C. A.; Migliari, S.; Fender, R. P.; Thompson, T. W. J.; van der Klis, M.; Mendez, R. Coupled radio and X-ray emission and evidence for discrete ejecta in the jets of SS 433 Published in: *The Astrophysical Journal*
- [8] Garofalo D., Evans D.A., Sambruna R.M. // *MNRAS*, 2010. – Vol. 406. – P. 975.
- [9] D. Garofalo, Retrograde versus Prograde Models of Accreting Black Holes, *Advances in Astronomy* Volume 2013 (2013), Article ID 213105.